Research Article   **Open Access**

The Role of Autonomic Nervous System on Right Ventricular Outflow Tract Tachycardia

Hung-Yu Chang[1,2], Li-Wei Lo[2,3,4*], Yu-Hui Chou[3], Wei-Lun Lin[2,3,4], Yenn-Jiang Lin[2,3,4], Wei-Hsian Yin[1,2], An-Ning Feng[1,2] and Shih-Ann Chen[2,3,4]

[1]Division of Cardiology, Cheng Hsin General Hospital, Taipei, Taiwan

[2]Faculty of Medicine, School of Medicine, National Yang Ming University, Taipei, Taiwan

[3]Division of Cardiology, Taipei Veterans General Hospital, Taipei, Taiwan

[4]Institute of Clinical Medicine and Cardiovascular Research Center, National Yang-Ming University, Taipei, Taiwan

*Corresponding author: Li-Wei Lo, Division of Cardiology, Taipei Veterans General Hospital, 201, Sec. 2, Shih-Pai Road, Taipei, Taiwan, Tel: +52 55 5729 6000; Fax: 886-2-2873-5656; E-mail: gyrus@ms65.hinet.net

Abstract

Background: Right ventricular outflow tract ventricular tachycardia (VT) and ventricular premature complexes (VPCs) are characterized as benign in entity with ECG morphology showing LBBB pattern and inferior axis. Pathogenic mechanisms in the genesis of RVOT VT/VPC remain largely unknown. We aimed to investigate the neural mechanism in RVOT VT/VPC in canine model.

Methods: Twelve mongrel dogs (13.7 ± 1.3 Kg, 5 male dogs) were studied through midline thoracotomies. High-frequency stimulation (HFS) was applied to the proximal pulmonary artery (PA) to induce RVOT VT/VPC. An EnSite Array and a mapping catheter were used for electroanatomical mapping. The RVOT and PA were surgically excised for immunohistochemistry studies, including tyrosine hydroxylase (TH) stain for sympathetic nerves and choline acetyltransferase (ChAT) stain for parasympathetic nerves.

Results: In nine (75%) out of twelve dogs, HFS of the proximal PA induced RVOT-VT/VPC. The density of TH-positive nerves was significantly higher than that of ChAT-positive nerves (6803 ± 700 *vs.* 670 ± 252 $\mu m^2/mm^2$, p<0.001). Moreover, the density of TH-positive nerves was also significantly higher in the VT/VPC origin sites than that in the non-origin sites (18044 ± 2866 *vs.* 5554 ± 565 $\mu m^2/mm^2$, p=0.002). Catheter ablation of the proximal PA eliminated the inducibility of RVOT VT/VPC successfully.

Conclusion: HFS of the proximal PA could induce RVOT VT/VPC. The sympathetic nerves were densely innervated to the origin of RVOT VT/VPC, indicating the critical role of sympathetic hyperactivity in the initiation and perpetuation of RVOT VT/VPC.

Introduction

Ventricular tachycardia (VT) arising from the right ventricular outflow tract (RVOT) is one of the most common types of idiopathic ventricular arrhythmias [1,2]. RVOT-VTs exhibit the following characteristics [2,3]: (1) they usually occur in patients without overt structural heart disease, (2) the surface 12-lead ECG typically shows left bundle branch block morphology and inferior axis, and (3) the tachycardia typically arises from a discrete area of the myocardium in the RVOT area.

Although pathogenic mechanisms in the genesis of RVOT-VT remained largely unknown, activation of sympathetic tone has been shown to play an important role in provoking as well as maintaining these arrhythmias. The frequency of ventricular arrhythmias is often increased during periods of wakefulness and activity, and they frequently disappear entirely during sleep [2,4]. They are sensitive to catecholamine infusion, and typically terminate in response to beta-blockers, calcium channel blockers, and adenosine [5,6]. Heart rate variability studies showed activation of sympathetic tone prior to the occurrence of these ventricular arrhythmias [7-9].

Sympathetic fibers of the ventromedial cardiac nerve (VMCN) and branches of ventrolateral cardiac nerve (VLCN) innervate the myocardium within the proximal pulmonary artery (PA) and the RVOT [10]. Recently, an animal model has been described for RVOT tachycardia by high-frequency stimulation (HFS) of the extravascular sympathetic nerves within the PA innervating the RVOT [11]. Similarly, HFS in the left pulmonary artery successfully induced RVOT-ventricular premature complexes (VPCs) and/or VT in a human model [12]. However, in both models, the mechanism whereby a discrete area of myocardium in the RVOT becomes arrhythmogenic is yet to be clarified. Thus, the aim of this study was to investigate the neural mechanism of RVOT ventricular arrhythmias by using HFS within the PA in adult mongrel canine model.

Materials and Methods

Animal preparation

The protocol for this study was approved by the Committee for Experiments on Animals of the Taipei Veteran General Hospital. The details were described in previous publications [13-15]. A total of twelve adult mongrel dogs (weight 15-25 Kg) were anesthetized with ketamine (10-20 mg/Kg) and sodium pentobarbital (30 mg/kg intravenous). No intervention is performed before experimental protocols in these dogs. All animals received a warming blanket to maintain the core body temperature at 36.5 ± 1.5°C. The arterial blood gas was checked hourly to keep a balanced acid-base status (pH 7.35-7.45) and oxygenation (SaO2>90% without hypercapnia). All dogs were ventilated with room air with a positive pressure respirator. Oxygen was administered to maintain SaO2>90%. Venous access was obtained by using the Seldinger technique from the femoral veins. An arterial access was set up at the right femoral artery for blood pressure and body temperature monitoring and blood sampling. The chest was opened via a mid-sternal thoracotomy and the heart was exposed after an incision through the pericardium.

Electroanatomic mapping, signal recording and analysis during sinus rhythm

The electroanatomic mapping was performed using a noncontact mapping system (NavX, St. Jude, MN, USA), consisted of a 9-French catheter with a multielectrode array (MEA) surrounding a 7.5 mL balloon mounted at the distal end. The detail has been described in our previous manuscript [14,16]. In brief, the MEA catheter was placed into the right ventricle via right or left femoral vein. The system located the three-dimensional position of the electrodes on any desired catheter relative to the MEA using a navigation signal. Navigation provided the means to define a model of the chamber anatomy and to track the position of a standard contact catheter within the chamber relative to labeled points of interest. Over 3,000 simultaneous virtual unipolar electrograms were mathematically reconstructed and displayed on the anatomical model, producing isopotential or isochronal color maps. Continuous recording of the RVOT global signals was obtained during the sinus rhythm. Raw data detected by the MEA was amplified and digitally transferred to a computer workstation.

A 4 mm-tip ablation catheter was inserted into the right ventricle and was also used to collect local bipolar ventricular signals during sinus rhythm with a point-by-point approach. All bipolar signals suitable for the frequency analysis and electrogram morphology analysis were exported for analysis.

Induction and identification of RVOT VT or ectopy

A quadripolar catheter was positioned in the right atrial appendage, and another 5-French decapolar circular catheter was positioned in the PA so as to contact the endovascular circumference of the PA. A 50 ms train of high frequency electrical stimulation with 200 Hz and 0.1 ms pulse duration (Grass Stimulator, S-88, Astro-Med Industrial Park, West Warwick, RI, USA) was applied at each of the bipolar pair of the circular catheter. Each train of HFS was coupled to right atrial pacing, and the coupling interval was adjusted so that the 50 ms train occurred after local ventricular activation and during the QRS interval of each cardiac cycle.

The reproducibility of the inducible ventricular ectopy and/or VT was confirmed by several times of HFS. After the induction of the monomorphic ventricular ectopy and/or VT with left bundle branch block-morphology and inferior axis, recording of the RVOT signals was obtained by the MEA catheter. The origin of the tachycardia, defined as the earliest ventricular activation site during monomorphic ventricular ectopy and/or VT, was determined by using noncontact mapping system. The substrate characteristics of this region were compared to the other region, and the tissue is sampled for detailed analysis.

Catheter ablation for proximal pulmonary artery

A 7-French 4 mm ablation catheter (BlazerTM II, Boston Scientific Corp., Natick, MA, USA) was placed at the epicardial site of the proximal PA opposite to the 5-French circular catheter by direct, manual manipulation. The region where ventricular ectopy and/or VT could be induced by HFS was ablated. Ablation was performed using the radiofrequency energy with maximal power 40-50 W and target temperature 50-55°C. Completeness of ablation was verified by elimination of inducible ventricular arrhythmia by applying the same high-frequency stimulation at the same regions.

Tissue sampling and immunohistochemistry study

After the experiment, nine whole-layered samples (1-2 cm 2 surface area for each sample) were collected from the origin of VAs; upper, middle and lower RVOT anterior free wall, posterior free wall and septum (Figure 1). The location of the sampling of each anatomic site was marked by a suture line in the center. Sections were excised parallel to the plane of pulmonary valves. All samples were fixed in 20% formalin before staining. Primary antibodies were then incubated overnight at 4°C. Antibodies for tyrosine hydroxylase (TH) were used to stain sympathetic nerves, whereas antibodies for choline acetyltransferase (ChAT) were used to stain parasympathetic nerves. After incubation, the slides were washed in Tris-buffered saline, and the appropriate secondary antibody was placed on the sections for 30 min. The sections were again washed in Tris-buffered saline, and the appropriate chromagen was added to each specimen. The specimens were then dehydrated in alcohol, mounted, and examined under light microscopy. The nerve bundle was confirmed by positive staining by the neurofilament-protein antibody. The TH and ChAT-positive portions within each sample were localized and the cross-sectional areas of these positive portions were measured.

Statistical analysis

Quantitative data were expressed as the mean value ± standard error (SE). The student's t-test was used for the comparisons between the continuous data and the Chi-square test and Pearson or Fisher's exact tests were used for the comparisons between categorical data. Statistical analysis was performed using SPSS Statistics 17.0 software (Chicago, Ill). All values were considered statistically significant at a two-tailed P value of less than 0.05.

Results

A total of 12 adult mongrel dogs (13.7 ± 1.3 kg, 5 male dogs) were included in the study. The MEA catheter was delivered in the RVOT in all dogs.
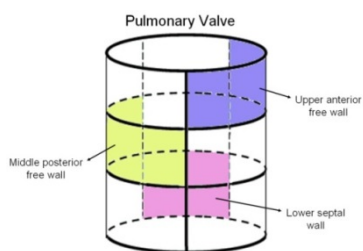
Figure 1: Right ventricular outflow tract was divided into 9 parts for tissue sampling and immunohistochemistry study.

Induction and identification of RVOT VT or ectopy

In nine (75%) out of twelve dogs, HFS of the proximal PA induced RVOT-VT/VPC, including 3 with RVOT VT and 6 with RVOT PVC (Figure 2). The origins of ventricular arrhythmias were identified by Ensite Array system with five originating from RVOT septal wall and three from RVOT posterior free wall and one from RVOT anterior free wall. Three dogs failed to induce VT/VPC through HFS up to max output (15 mV). Figure 3 shows an example of electroanatomical mapping for the posterior free wall origin of inducible RVOT-VT.

Catheter ablation for proximal PA

Catheter ablation of the proximal PA was performed using direct, manual manipulation from the epicardial site and was verified by the non-inducibility of the same arrhythmia with the maximal output of HFS. Ablation time was 173 ± 21 s. Target temperature of 50-55 could be achieved in all animals. No ventricular tachyarrhythmias were induced during ablation. No steam pop happened during ablation. In all dogs, radiofrequency ablation successfully eliminated the inducibility of RVOT VT/VPC by HFS.

Figure 2: Two examples of inducible RVOT VT/VPC by high frequency stimulation of pulmonary artery. A 50 ms of high frequency stimulation train was coupled to right atrial pacing, and the coupling interval was adjusted so that the 50 ms train occurred after local ventricular activation and during the QRS interval of each cardiac cycle.

Figure 3: Example of electroanatomical mapping for the origin of inducible RVOT VT. The isopotential map of RVOT is shown. White color in the figure indicated that the earliest VT activation site was locating at the lower posterior free wall of RVOT. The virtual unipolar electrogram (at red asterisk site) revealed QS pattern, indicating the origin of the tachycardia.

Immunohistochemistry study in detection of regional neuronal distribution

Immunohistochemical staining of RVOT demonstrated that the density of TH-positive nerves was significantly higher than that of ChAT-positive nerves (6803 ± 700 $vs.$ 670 ± 252 $\mu m^2/mm^2$, p<0.001). The cross-sectional area percentage was 0.52 ± 0.18% of TH-positive nerves, which was also significantly higher than that of ChAT-positive nerves (0.06 ± 0.05%, p<0.001). The regional TH-positive and ChAT-positive nerves analysis of different RVOT sites is shown in Figure 4. In all regions, the densities of TH-positive nerves were significantly higher than those of ChAT-positive nerves. There were no significant differences among the densities of TH-positive nerves and the densities of ChAT-positive nerves of the different RVOT sites.

The density of TH-positive nerves was also significantly higher in the VT/VPC origin sites than that in the non-origin sites (18044 ± 2866 $\mu m^2/mm^2$ $vs.$ 5554 ± 565 $\mu m^2/mm^2$, p=0.002) (Figure 5). Figure 6 shows examples of TH, ChAT and neurofilament stains of the nerve components at RVOT VT/VPC origin sites and non-origin RVOT sites. The distribution of nerve bundle was confirmed by positive staining with neurofilament-protein antibody. The neural density of TH-positive component at VPC/VT origin was significantly higher than that of non-origin site, whereas the neural density of ChAT-positive component was limited and did not differ between two sites.

Discussion

Main findings

The present study demonstrated an animal model of idiopathic RVOT VT/VPC by HFS of the proximal PA. Our electrophysiological study showed that HFS at the PA without capturing ventricular myocardium could induce RVOT ventricular arrhythmias, and immunohistochemistry study showed the increasing sympathetic nerve innervations of RVOT, especially at the site of arrhythmogenic origin. Our study implied the autonomic activity is related to the generation of RVOT ventricular arrhythmia and focal sympathetic hyperinnervation in RVOT might explain the underlying mechanism of this arrhythmia.
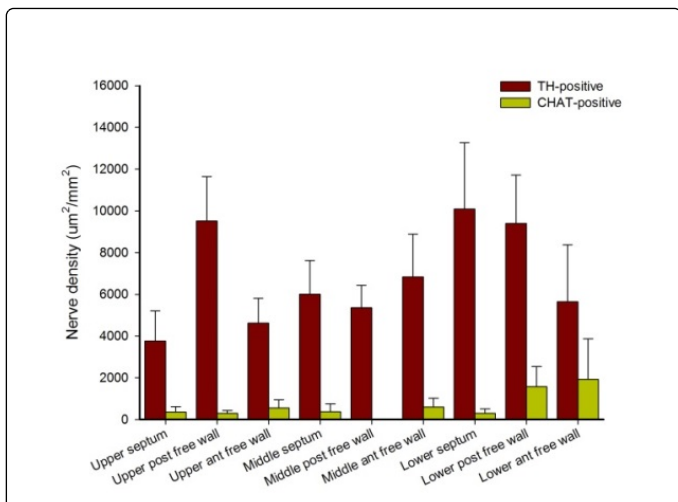
Figure 4: Regional analysis of RVOT immunohistochemical staining by TH for sympathetic nerves and ChAT for parasympathetic nerves. The densities of TH-positive nerves are significantly higher than those of ChAT-positive nerves.
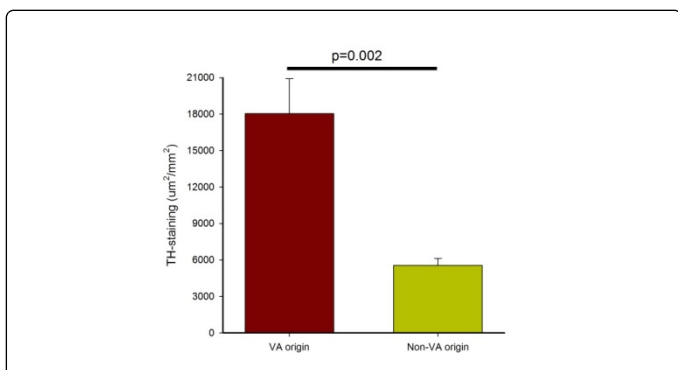

Figure 5: Comparison of immunohistochemical staining of TH positive nerve density showed that the density of TH-positive nerves was significantly higher in the VT/VPC origin sites than that in the non-origin sites.
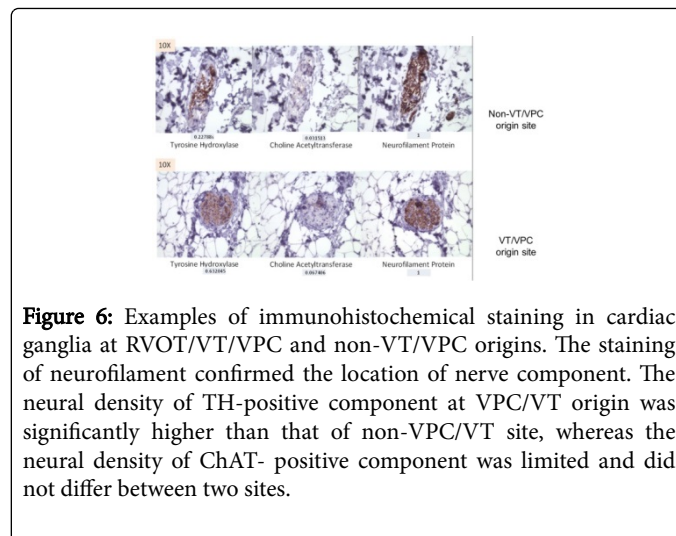

Figure 6: Examples of immunohistochemical staining in cardiac ganglia at RVOT/VT/VPC and non-VT/VPC origins. The staining of neurofilament confirmed the location of nerve component. The neural density of TH-positive component at VPC/VT origin was significantly higher than that of non-VPC/VT site, whereas the neural density of ChAT- positive component was limited and did not differ between two sites.

Neuronal distribution and the associated embryonic role of RVOT in the generation of ventricular arrhythmias

Sympathetic activation has been demonstrated pivotal roles in initiation and maintenance of RVOT VT/VPC clinically. Sympathetic arousal prior to the attack of ventricular arrhythmias have been detected by using heart rate variability [7-9]. However, the detailed role of sympathetic nerve in the generation of RVOT VT/VPC was not clearly clarified. The present study demonstrated indirect evidence of sympathetic nerve in the arrhythmogenesis of RVOT VT/VPC. Increased density of TH positive sympathetic nerve ending within RVOT, especially the origin of VT/VPC, implied the pivotal role of sympathetic nerve in the generation of VT/VPC. Myocardial substrates overlying RVOT and proximal PA sleeve are innervated by sympathetic fibers of the ventromedial cardiac nerve (VMCN) and branches of ventrolateral cardiac nerve (VLCN) [10]. The distribution of sympathetic fiber results in the non-uniform distribution of RVOT VT/VPC. Additionally, the response of RVOT VT/VPC to catecholamine, which was usually attenuated by beta-blocker, calcium channel blockers and adenosine [5,6], provided the indirect evidence of sympathetic tone in the arrhythmogenesis of RVOT VA. That RVOT VT/VPC could be eliminated by catheter ablation also reflected that sympathetic denervation could be a useful strategy for elimination of VT/VPC originated from RVOT.

Conclusions

HFS of the proximal PA could induce RVOT VT/VPC. The innervations of sympathetic nerve were non-uniform and well correlated to the origin of RVOT VT/VPC. Elimination of RVOT VT/VPC by catheter ablation implied the denervation of sympathetic distribution decreased the spontaneous triggers. The present results shed insight into the neural mechanism in contribution to RVOT VT/VPC, indicating the critical role of sympathetic hyperactivity in the initiation and perpetuation of RVOT VT/VPC.

Acknowledgement

Induction of RVOT VA by HFS of proximal PA

Idiopathic VT in structural normal heart is mostly originated from RVOT. Though it was considered as benign in characteristics, previous studies reported the associations between idiopathic RVOT VT and VPC related cardiomyopathy and idiopathic ventricular fibrillation. Zhou et al. [11] firstly introduced the animal model of idiopathic RVOT VT by HFS of proximal PA. In the present study, we confirmed the efficacy of HFS of proximal PA in generation of RVOT VT/VPC. Pacing over the PA during the ventricular refractory period suggested that the RVOT VT/VPC was not generated by capture of sleeves within PA. The development of RVOT ventricular arrhythmia could be explained by the capture of nerve fiber distributed epicardially surrounding the PA. Moreover, RVOT VT/VPC was developed during HFS rather than low frequency stimulation suggested that HFS increased neural firing, which could accentuate the neurotransmitter within the nerve ending and contributed the development of RVOT VT/VPC.

References

1. NakagawaM, Takahashi N, Nobe S, Ichinose M, Ooie T, et al. (2002) Gender differences in various types of idiopathic ventricular tachycardia. J Cardiovasc Electrophysiol 13: 633-638.

2. Lerman B, Stein K, Markowitz S, Mittal S, Iwai S (2004) Ventricular tachycardia in patients with structurally normal hearts. In: Zipes DP, Jalife J, eds. Cardiac Electrophysiology: From Cell to Bedside (4thedition.) Saunders, Philadelphia, USA. pp: 668-682.

3. Cole C, Marrouche N, Natale A (2002) Evaluation and management of ventricular outflow tract tachycardias. Card Electrophysiol Rev 6: 442-447.

4. Mont L, Seixas T, Brugada P, Brugada J, Simonis F, et al. (1991) Clinical and electrophysiologic characteristics of exercise-related idiopathic ventricular tachycardia. Am J Cardiol 68: 897-900.

5. Iwai S, Cantillon DJ, Kim RJ, Markowitz SM, Mittal S, et al. (2006) Right and left ventricular outflow tract tachycardias: Evidence for a common electrophysiologic mechanism. J Cardiovasc Electrophysiol 17: 1052-1058.

6. Kim RJ, Iwai S, Markowitz SM, Shah BK, Stein KM, et al. (2007) Clinical and electrophysiological spectrum of idiopathic ventricular outflow tract arrhythmias. J Am Coll Cardiol 49: 2035-2043.

7. Hayashi H, Fujiki A, Tani M, Mizumaki K, Shimono M, et al. (1997) Role of sympathovagal balance in the initiation of idiopathic ventricular tachycardia originating from right ventricular outflow tract. pacing Clin Electrophysiol 20: 2371-2377.

8. Yoshida A, Inoue T, Ohnishi Y, Yokoyama M (1998) Heart rate variability before spontaneous episodes of ventricular tachycardia originating from right ventricular outflow tract in patients without organic heart disease. Jpn Circ J 62: 745-749.

9. Zimmermann M (2005) Sympathovagal balance prior to onset of repetitive monomorphic idiopathic ventricular tachycardia. Pacing Clin Electrophysiol 28: 163-167.

10. Randall WC, Armour JA, Geis WP, Lippincott DB (1972) Regional cardiac distribution of the sympathetic nerves. Fed Proc 31: 1199-1208.

11. Zhou J, Scherlag BJ, Yamanashi W, Wu R, Huang Y, et al. (2006) Experimental model simulating right ventricular outflow tract tachycardia: A novel technique to initiate RVOT-VT. J Cardiovasc Electrophysiol 17: 771-775.

12. Hasdemir C, Alp A, Aydin M, Can LH (2009) Human model simulating right ventricular outflow tract tachycardia by high-frequency stimulation in the left pulmonary artery: autonomics and idiopathic ventricular arrhythmias. J Cardiovasc Electrophysiol 20: 759-763.

13. Yamada S, Lo LW, Chou YH, Lin WL, Chang SL, et al. (2017) Beneficial Effect of Renal Denervation on Ventricular Premature Complex Induced Cardiomyopathy. J Am Heart Assoc 6: e004479.

14. Chang HY, Lo LW, Chou YH, Lin WL, Lin YJ, et al. (2016) Effect of vagotomy on the activity of cardiac autonomic ganglia: Insight from left atrial high density frequency mapping. Int J Cardiol 220: 435-439.

15. Lo LW, Chang HY, Scherlag BJ, Lin YJ, Chou YH, et al. (2016) Temporary Suppression of Cardiac Ganglionated Plexi Leads to Long-Term Suppression of Atrial Fibrillation: Evidence of Early Autonomic Intervention to Break the Vicious Cycle of "AF Begets AF". J Am Heart Assoc 5: e003309.

16. Lo LW, Chiou CW, Lin YJ, Lee SH, Chen SA (2011) Neural mechanism of atrial fibrillation: insight from global high density frequency mapping. J Cardiovasc Electrophysiol 22: 1049-1056.